ELSEVIER

NeuroImage

www.elsevier.com/locate/ynimg
NeuroImage 32 (2006) 978 – 987

EEG oscillations and recognition memory: Theta correlates of memory retrieval and decision making

Joshua Jacobs,[a] Grace Hwang,[b] Tim Curran,[c] and Michael J. Kahana[b,*]

[a]*Neuroscience Graduate Group, University of Pennsylvania, Philadelphia, PA 19104, USA*
[b]*Department of Psychology, University of Pennsylvania, 3401 Walnut Street, Room 303C, Philadelphia, PA 19104, USA*
[c]*Department of Psychology, University of Colorado at Boulder, Boulder, CO 80309, USA*

Received 29 December 2005; revised 7 February 2006; accepted 8 February 2006
Available online 12 July 2006

Studies of memory retrieval have identified electroencephalographic (EEG) correlates of a test item's old–new status, reaction time, and memory load. In the current study, we used a multivariate analysis to disentangle the effects of these correlated variables. During retrieval, power of left-parietal theta (4–8 Hz) oscillations increased in proportion to how well a test item was remembered, and theta in central regions correlated with decision making. We also studied how these oscillatory dynamics complemented event-related potentials. These findings are the first to demonstrate that distinct patterns of theta oscillations can simultaneously relate to different aspects of behavior.

Keywords: Theta; EEG oscillations; Recognition memory; Decision making; Working memory; Gamma

Introduction

Understanding the functional role of human electroencephalographic (EEG) oscillations is complicated by the fact that oscillatory patterns have been observed to correlate with multiple experimental manipulations. For example, in recent memory studies, theta (4–8 Hz) oscillations correlated with memory load (Jensen and Tesche, 2002), task difficulty (Gevins et al., 1997), error processing (Luu et al., 2004), stimulus type (Hwang et al., 2005), and recognition of previously viewed stimuli (Klimesch et al., 2000; Klimesch et al., 2006). Oscillations at other frequencies, in addition to theta, have also been observed to vary with task variables: Alpha (9–12 Hz) power was observed to increase with memory load in simple working-memory tasks (Jensen et al., 2002) but to decrease as memory load increased during more demanding tasks (Gevins et al., 1997). Gamma (30–60 Hz) power has been observed to correlate with memory load (Howard et al., 2003), stimulus novelty (Gruber and Matthias, 2005), attention (Tallon-Baudry et al., 2005), and reaction time (Gonzalez Andino et al., 2005; Jokeit and Makeig, 1994). Similarly, studies of spatial memory have reported increased theta power during learning of long as compared to short mazes, movement as compared to stillness, retrieval as compared to encoding, and searching for randomly placed targets as compared to searching for fixed-location landmarks (Kahana et al., 1999; Caplan et al., 2001, 2003; Ekstrom et al., 2005; de Araujo et al., 2002). One recent study (Bastiaansen et al., 2005) directly illustrates the complexity of determining how EEG oscillations correlate with task variables: during visual word presentation, left-posterior theta power simultaneously correlated with both word length and whether a word served a primarily semantic (e.g., nouns and verbs) or a primarily syntactic (e.g., prepositions and conjunctions) function. Consistent with these reports, recent reviews (Buzsáki, 2002; Bastiaansen and Hagoort, 2003; Kahana et al., 2001) describe a diverse array of relations between oscillations and behavior, with no single pattern emerging clearly.

One difficulty in using memory tasks to study EEG oscillations is that an experimental manipulation may cause a change in response accuracy or reaction time (RT). In these cases, it can be unclear if an observed EEG pattern is a direct correlate of the manipulation itself, or if it is more closely related to the accuracy–RT change. An example of this is the linear relation between study list length and RT in working-memory tasks (Sternberg, 1966). This list-length–RT relation makes it difficult to distinguish whether an EEG pattern that correlates with list length is actually a direct result of an increase in RT. In addition to list length, other experimental manipulations, such as the position of a memory probe in a just-presented list (Forrin and Cunningham, 1973), also influence RT, thus creating more potential confounds. This type of issue has surfaced in recent EEG publications, where it has been observed that theta power increased during experimental manipulations that raised task difficulty, such as increases in stimulus complexity (Gevins et al., 1997) or memory load (Jensen and Tesche, 2002). Although these EEG patterns could be interpreted

* Corresponding author. Fax: +1 215 746 3848.
E-mail address: kahana@psych.upenn.edu (M.J. Kahana).
Available online on ScienceDirect (www.sciencedirect.com).

1053-8119/$ - see front matter © 2006 Elsevier Inc. All rights reserved.
doi:10.1016/j.neuroimage.2006.02.018

as direct correlates of stimulus changes, another interpretation is that these patterns were related to a more general phenomenon: increased RT.

To address these concerns, we considered the possibility that EEG oscillations simultaneously relate to multiple aspects of behavior. Thus, we designed a framework to analyze how power of EEG oscillations simultaneously correlates with task variables (experimental manipulations and RT) in a working-memory task. This approach has two main benefits: First, by simultaneously analyzing how task variables relate to oscillatory power, it is possible to distinguish which variable best predicts an oscillatory pattern. Second, our framework is capable of identifying oscillatory patterns that correlate with multiple task variables.

Because working-memory studies have found EEG oscillations to be correlated with a wide range of variables, and because the behavioral data in such studies are well characterized (Sternberg, 1975), we sought to simultaneously examine the relation of EEG oscillatory power—across a broad range of frequencies, after-probe latencies, and electrodes—with each of the major variables that characterize working-memory performance. Subjects performed the Sternberg working-memory task while EEG was recorded at 129 scalp electrodes. On each trial, subjects were asked to judge whether a test probe was a member of a just-presented list of consonants. We varied the number of list items, whether the probe matched one of the studied items, and (if so) the position of the probe in the list. We fit a multivariate linear model to predict EEG oscillatory activity after probe using details of each presented list and RT. An analysis of this model identified oscillatory correlates of probe old–new status, RT, memory load, and study–test lag.

Methods

Participants

Eighteen right-handed University of Colorado students (6 males and 12 females) were paid to participate in two experimental sessions. All subjects were between the ages of 19 and 29. Two subjects participated in only a single session because of technical difficulties.

Procedure

In each of 576 trials, which were distributed across two sessions on different days, subjects viewed a list of 2, 4, or 6 consonants followed by a test probe. All interstimulus intervals (ISIs) were randomly jittered to decorrelate evoked activity across stimulus presentations. Trials began with presentation of a fixation cross for 1 s, followed by a 100–300-ms ISI. Each consonant was then presented for 750 ms, followed by a 200–300-ms ISI. The final list item was followed by a 200–300-ms ISI, and then subjects were presented with a memory probe, shown in red (all other items were displayed in white against a black background). In response to the probe, subjects were asked to press a key on a keyboard indicating as quickly as possible if the probe was a *target* (i.e., an item presented on the study list) or a *lure* (i.e., an item that was not on the study list). The specific keys used for indicating target and lure responses were counterbalanced across subjects. List length, probe target–lure status, and (for target trials) probe position were determined randomly for each trial. Both response accuracy and RT were recorded.

Scalp voltages were measured with a 129-channel Geodesic Sensor Net connected to an AC-coupled, high-input-impedance amplifier (200 MΩ, Net Amps™, Electrical Geodesics, Inc., Eugene, OR). Amplified analog voltages (0.1–100 Hz bandpass, −3 dB) were sampled at 500 Hz. Individual sensors were adjusted until impedances were less than 50 kΩ. EEG was measured with respect to an average reference. The average reference was computed by subtracting the mean voltage across all electrodes from the voltage measured at each individual electrode (Dien, 1998). Trials in which a blink was recorded within 1000 ms of the probe were discarded (blinks were located by monitoring electro-oculogram for voltages over 70 μV). Overall, 4% of trials were discarded because of blinks.

Oscillatory analyses

A Morlet wavelet transform (6 cycles) was used to compute EEG oscillatory power at 9 time points after each probe (0, 100, . . . , 800 ms) for 21 logarithmically spaced frequencies between 2 and 64 Hz ($2^{x/4}$ Hz for $x \in 4, \ldots, 24$). We then converted each subject's log-transformed power P in each trial i to a Z score at each frequency f, time point t, and electrode e:

$$Z_{(f,t,e)}(i) = \frac{P_{(f,t,e)}(i) - \mu_{(f,t,e)}}{\sigma_{(f,t,e)}} \quad (1)$$

$\mu_{(f,t,e)}$ and $\sigma_{(f,t,e)}$ are the mean and standard deviation, respectively, of the subject's log-transformed oscillatory power at frequency f, time point t, and electrode e across all trials. Eq. (1) was computed separately for each subject, and then all subjects' trials were combined into a single data set.

We next used a multivariate linear model to characterize the relation between oscillatory power and task variables at each frequency, time point, and electrode. Fitting data from only correct trials (errors were rare), we used ordinary least squares (OLS) to estimate values for the βs in the following model:

$$Z_{(f,t,e)} = \beta^{\mathrm{TL}}_{(f,t,e)}\mathrm{TL} + \beta^{\mathrm{RTQ}}_{(f,t,e)}\mathrm{RTQ} + \beta^{\mathrm{LL}}_{(f,t,e)}\mathrm{LL} + \beta^{\mathrm{Lag}}_{(f,t,e)}\mathrm{Lag} + \beta^{\mathrm{TLC}}_{(f,t,e)}\mathrm{TLC} + \epsilon \quad (2)$$

TL is a dummy variable indicating whether each trial's probe is target (1) or lure (0). RTQ indicates each trial's RT quartile (1 = fastest responses, 4 = slowest). To compute RTQ, RTs from each trial were binned by rank into quartiles individually for each subject. This procedure ensures that fast- and slow-responding subjects contribute equally to each RTQ label, to allow us to study relative RT changes. LL indicates each trial's study list length. Lag indicates how recently the probe was studied. In target trials, Lag is the number of stimuli between the probe's study presentation and the end of the study list. In lure trials, Lag is equal to LL.

Finally, TLC (target–lure confidence) is a variable introduced to represent the interaction between TL and RTQ. Specifically, TLC combines TL and RTQ to quantify the match between the test probe and memory of the just-presented list. Given the well-documented correlation between RT and response confidence (Murdock, 1974), we expected fast target responses when subjects were confident that they had previously viewed the probe—an indication that the probe closely matched their memory of a list stimulus. Inversely, we expected fast lure responses when subjects were confident they had not

viewed the probe, indicating that the probe was very different from their memory of list stimuli. We expected slower responses when there was a moderate degree of match between the probe memory of the list. TLC has values between 1 and 4 for the four values of RTQ for lure responses, ordered from fastest to slowest, and between 5 and 8 for the four values of RTQ for target responses, ordered from slowest to fastest. Thus, an EEG pattern that correlates with TLC indicates the degree of match between the probe and the memory of the just-presented list.

We Z-transformed the computed values of the task variables, obviating the need for a constant term in Eq. (2). Positive values of β^{TL}, β^{RTQ}, β^{LL}, β^{Lag}, and β^{TLC} indicate increased oscillatory power in trials with target probes, slow responses, long lists, probes for recently viewed stimuli, and high memory confidence, respectively. ϵ indicates the residual from the linear model. Topographic plots were created with the topoplot function from EEGLAB (Delorme and Makeig, 2004).

Correcting for multiple comparisons

Since Eq. (2) is applied at a number of frequencies, time points, and electrodes, it was necessary to adjust our significance threshold to control the number of times we falsely rejected the hypothesis that β was 0. Each fit of the model in Eq. (2) resulted in five P values (one for each β); the model was fitted at each of 129 electrodes, 8 after-probe time points, and 21 frequencies, resulting in ($5 \times 129 \times 8 \times 21$) 108,360 statistical comparisons. We analyzed the resulting distribution of P values with the False Discovery Rate (FDR) procedure (Genovese et al., 2002) to compute a P threshold of 0.0039 that sets the rate of falsely rejected null hypotheses to 5%. This procedure ensures a less than 5% rate (on average) of false positives among any null hypotheses we reject at $P < 0.0039$. In the accompanying figures, we plot β as 0 (green) when the corresponding $P \geq 0.0039$, meaning that colored (e.g., red or blue) points on plots indicate that $P < 0.0039$. Thus, the FDR-determined P threshold indicates that a colored data point has a ≥95% chance of being a correct rejection of the null hypothesis and a <5% chance of being a false positive.

Results

RT increased approximately linearly as list length increased from 2 to 6 items (627 ± 26 ms, 678 ± 27 ms, and 736 ± 31 ms for list lengths 2, 4, and 6, respectively). Error rates showed a similar increase with list length (2.7% ± 0.5%, 5.2% ± 1%, and 10.3% ± 1% for list lengths 2, 4, and 6, respectively). This pattern is in agreement with previous observations (Sternberg, 1966). The overall high level of accuracy led us to discard trials containing incorrect responses. The mean RTs of trials with each RTQ label were 498 ± 16 ms, 589 ± 22 ms, 682 ± 28 ms, and 805 ± 42 ms, ordered from fastest to slowest. Behavioral statistics were calculated across subjects and reported as mean ± standard error.

Fig. 1 summarizes the results of our regression model (Eq. (2)) at various electrodes. In subsequent sections, we focus on detailing the patterns that were robust at a range of electrodes, frequencies, and time points. These included β^{TL} and/or β^{TLC}, which was positive at ~4 Hz, ~300–800 ms after probe in the left-parietal region (see Figs. 1B–D). β^{RTQ} was positive at central electrodes at ~7 Hz, ~500–800 ms after probe (see Fig. 1H), and at widespread electrodes at ~32 Hz, 0–400 ms after probe (see Figs. 1A–D, G–J). β^{LL} was negative at ~3–7 Hz, 0–400 ms after probe at widespread electrodes (see Figs. 1A, B, D–J). Finally, β^{Lag} was negative at 2 Hz, 0–400 ms after probe at left-parietal electrodes (see Figs. 1C–E).

Oscillatory correlates of memory recognition (TL and TLC)

We observed increased left-parietal theta power following target probes (indicated by positive values of β^{TL} in Figs. 1B–D). To further illustrate the theta target–lure phenomenon, Fig. 2A plots left-parietal theta (4 Hz) power for the fastest and slowest quartiles of target and lure trials. At 300 ms after probe, theta power was greater following target probes than following lures. Furthermore, this pattern was magnified in trials when subjects responded quickly—a finding that inspired us to create the TLC variable to directly study the interaction between TL and RTQ.

At a left-parietal electrode (Fig. 1D), we observed that β^{TLC} but not β^{TL} was positive at 4 Hz, 300 ms after probe, indicating that theta power at this time point is best predicted by the degree of match between the probe and memory contents. However, at 4 Hz, 400–800 ms after probe, β^{TL} but not β^{TLC} was positive, indicating that theta power is best predicted by whether the probe is a target or lure (TL) rather than by TLC. Fig. 2B topographically plots β^{TLC} at 4 Hz, 300 ms after probe, illustrating that the effect localizes to the left-parietal region. Likewise, Fig. 2C topographically plots β^{TL} at 4 Hz, 500 ms after probe.

Oscillatory correlates of reaction time (RTQ) in decision making

Fig. 1H indicates that β^{RTQ} at a central electrode is positive at ~4–8 Hz, ~400–900 ms after probe, indicating increased theta power in trials in which subjects responded slowly. To further illustrate this relation, Figs. 3A and B plot the time courses of theta (7 Hz) power at this electrode, aligned to the probe and response, respectively. Fig. 3A shows that theta power consistently increased after the probe's onset, and remained elevated for a duration proportional to RTQ. Fig. 3B shows that theta power began to decrease shortly before the response. Fig. 3C topographically plots β^{RTQ} at 7 Hz, 600 ms after probe, indicating that the theta–RTQ relation localized to central electrodes. Beta and gamma oscillations also correlated with RTQ (see Fig. 1H): 16–32 Hz power was elevated at ~0–400 ms after probe in trials with slow RTs, as indicated by positive values of β^{RTQ}. Fig. 3D plots β^{RTQ} at 32 Hz, 100 ms after probe, indicating that this phenomenon is present at widespread electrodes.

Oscillatory correlates of memory load (LL)

Figs. 1D–J illustrate negative values of β^{LL} at 4–8 Hz, 100–500 ms after probe, indicating increased theta power for short compared to long lists. This relation is detailed in Fig. 4A, where 4-Hz power at a right-parietal electrode, 100 ms after probe, is plotted as a function of list length and lag. Fig. 4B plots the topography of β^{LL} at 4 Hz, 100 ms after probe, illustrating negative relations between theta power and LL at widespread electrodes. This pattern occurs so early after the probe's onset (0–100 ms after

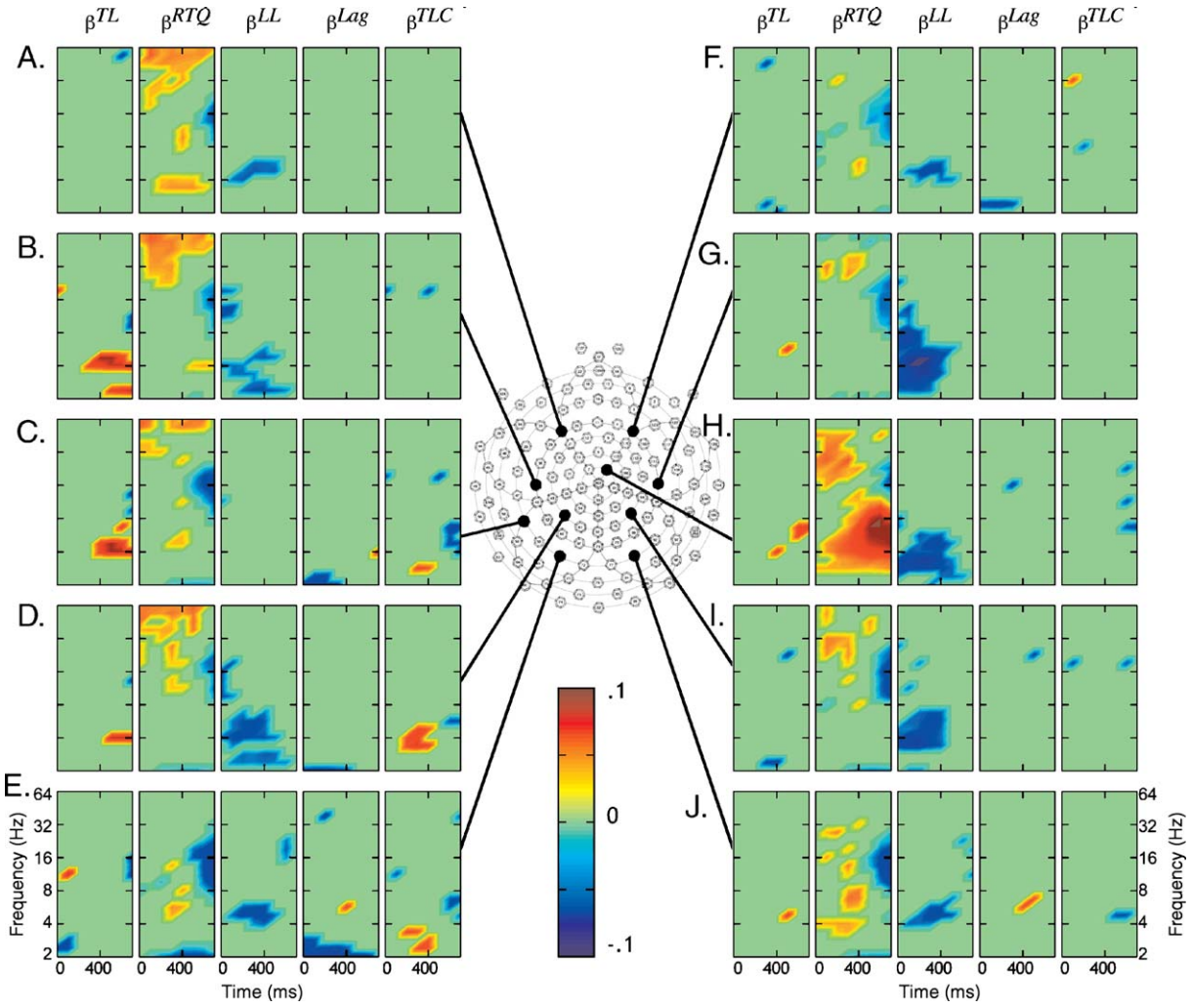

Fig. 1. Regression analysis of oscillatory correlates of behavior. At each electrode, positive values for β^{TL}, β^{RTQ}, β^{LL}, β^{Lag}, and β^{TLC} indicate increased oscillatory power in trials with target probes, slow responses, long lists, probes for recently viewed items, and high memory confidence, respectively. Electrode positions are indicated by position on electrode map (nose is up). βs are plotted as a function of frequency and after-probe time point. βs with an associated $P \geq 0.0039$ are plotted as 0 (green). (A) Electrode 25 (F3). (B) Electrode 42 (C5). (C) Electrode 51 (TP7). (D) Electrode 53 (P3). (E) Electrode 66 (PO7). (F) Electrode 124 (F4). (G) Electrode 104 (C6). (H) Electrode 107 (immediately right-anterior to CZ). (I) Electrode 87 (P4). (J) Electrode 85 (PO8).

probe) that it probably relates to maintaining the studied list in memory rather than to probe processing.

Oscillatory correlates of probe position (Lag)

Figs. 1C–E describe negative values for β^{Lag} at 2 Hz, indicating increased delta power following probes for recently viewed items. Fig. 4C details this relation by plotting 2-Hz power as a function of lag at PO7. Fig. 4D plots the topography of β^{Lag} at 2 Hz, 300 ms after probe, indicating that this pattern localized to the left-occipital region.

Distinguishing oscillatory and event-related potential (ERP) correlates of behavior

Event-related potential (ERP) memory studies have reported a left-parietal voltage increase following presentation of target probes (Friedman and Johnson, 2000). Since the time course and topography of this phenomenon are similar to the β^{TL} patterns we observed (Fig. 2), we were interested in determining if these phenomena were directly related. Thus, we designed a framework to distinguish oscillatory and ERP correlates of task variables. First, we performed dual univariate regressions to study how oscillatory power and probe-evoked voltage related independently to a task variable:

$$Y = \beta^{pow}_{(f,t,e)} \mathrm{pow}_{(f,t,e)} + \epsilon \quad (3)$$

$$Y = \beta^{ERP}_{(t,e)} \mathrm{ERP}_{(t,e)} + \epsilon. \quad (4)$$

Y is a placeholder for one of the task variables described above. Indices f, t, and e represent the frequency, after-probe time point, and electrode of interest. $\mathrm{ERP}_{(t,e)}$ indicates the baseline-corrected, Z-transformed voltage at after-probe time point t. Voltage is baseline corrected to the average voltage −100–0 ms relative to the probe. Each subject's data were individually Z-transformed and

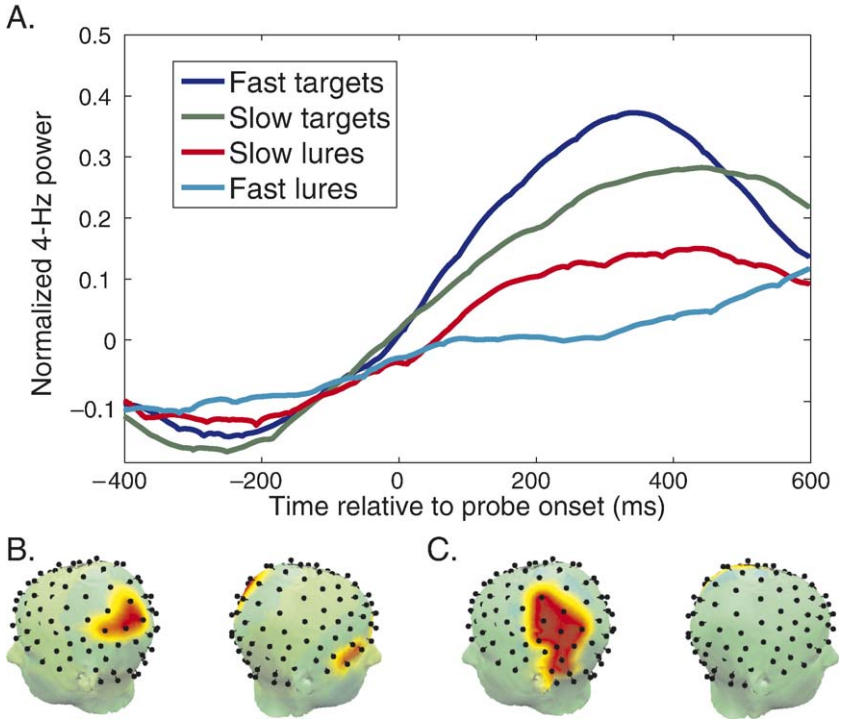

Fig. 2. Relation between probe target–lure status (TL) and left-parietal theta power. (A) Normalized after-probe theta (4 Hz) power at a left-parietal electrode (P3) for the fastest and slowest quartiles of responses, for targets and lures. Power at each time point for each quartile is normalized (Z-transformation) relative to the distribution of power values at stimulus onset (0 ms). (B) Topographic plot of β^{TLC} at 4 Hz, 300 ms after probe. (C) Topographic plot of β^{TL} at 4 Hz, 500 ms after probe. In panels B and C, βs with an associated $P \geq 0.0039$ are plotted as 0 (green).

then combined into a single dataset. Thus, the regression-determined β^{ERP} and β^{pow} indicate Y's independent relations with oscillatory power and evoked voltage, respectively.

To quantify the nature of any correlations between the respective relations of evoked voltage and oscillatory power to task variables, we performed a bivariate regression to use these variables simultaneously to predict task variable Y:

$$Y = \beta^{\mathrm{ERP\_bi}}_{(f,t,e)}\mathrm{ERP}_{(t,e)} + \beta^{\mathrm{pow\_bi}}_{(f,t,e)}\mathrm{pow}_{(f,t,e)} + \epsilon. \quad (5)$$

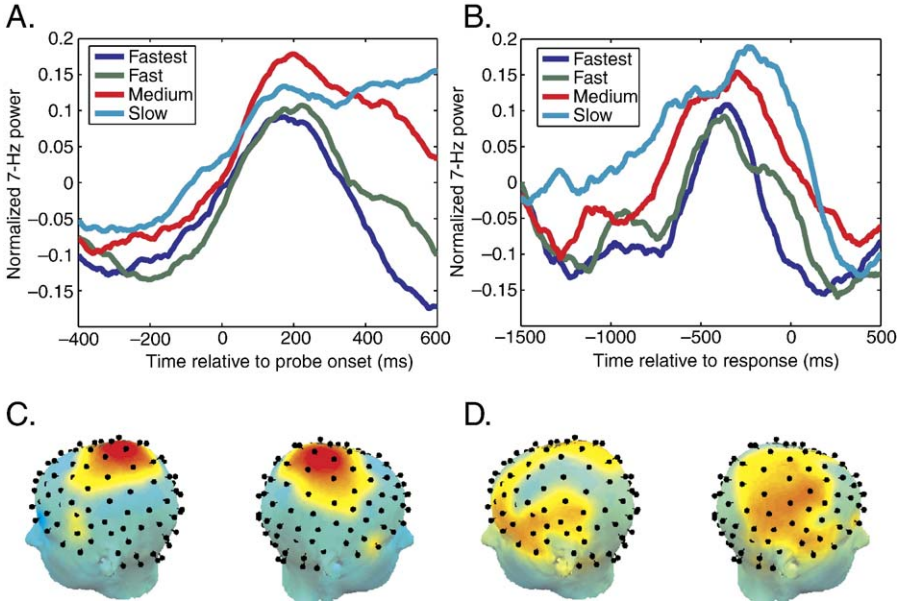

Fig. 3. EEG oscillations and reaction time (RTQ). (A) Theta (7 Hz) power at a central electrode (107, immediately right-anterior to CZ), aligned to the probe's onset, for trials with different RTQ labels. (B) Theta (7 Hz) power at this same electrode aligned to subject's response. In panels A and B, power is Z-transformed relative to 0 ms. (C) Topographic plot of β^{RTQ} at 7 Hz, 600 ms after probe. (D) Topographic plot of β^{RTQ} at 32 Hz, 100 ms after probe. In C and D, β^{RTQ} with an associated $P \geq 0.0039$ is plotted as 0 (green).

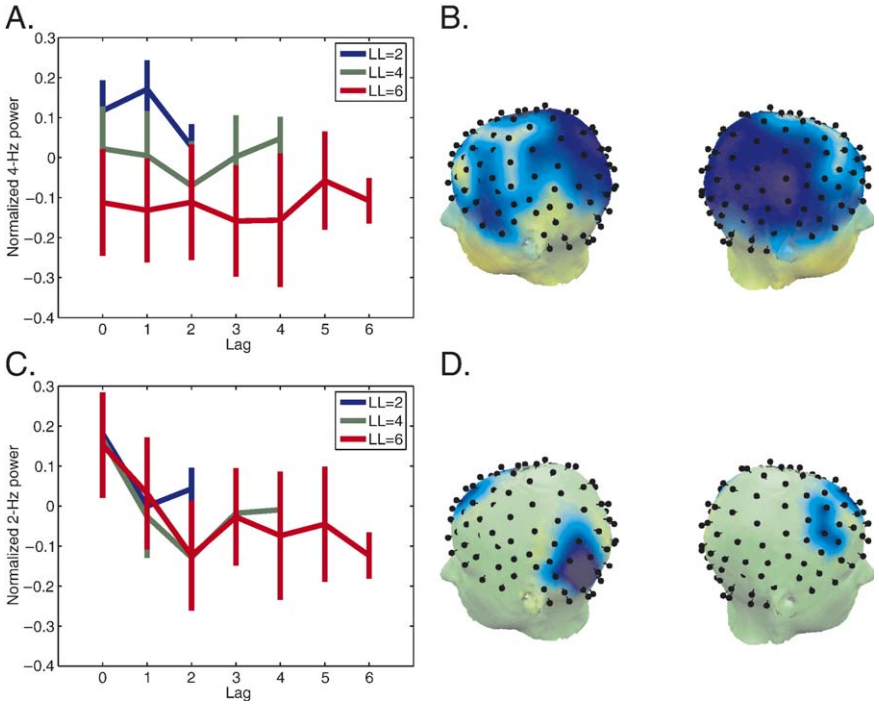

Fig. 4. Oscillatory power as a function of list length (LL) and lag since first probe presentation (Lag). (A) Theta (4 Hz) power 100 ms after probe at electrode 79 (immediately medial to P4). Power is plotted as a function of lag since first probe presentation, grouped by list-length. (B) β^{Lag} at 4 Hz, 100 ms after probe, plotted topographically. (C) Delta (2 Hz) power 300 ms after probe at PO7. (D) β^{Lag} at 2 Hz, 300 ms after probe, plotted topographically. In panels A and C, error bars denote 95% confidence intervals. In panels B and D, βs with an associated $P \geq 0.0039$ are plotted as 0 (green).

To study how ERPs and oscillatory power relate to TL, we compared the regression-determined βs from Eqs. (3) and (4) to those from Eq. (5), substituting TL for *Y*. To the extent that $\beta^{\mathrm{ERP\_bi}}_{(f,t,e)} \neq \beta^{\mathrm{ERP}}_{(t,e)}$, or $\beta^{\mathrm{pow\_bi}}_{(f,t,e)} \neq \beta^{\mathrm{pow}}_{(f,t,e)}$, then oscillatory power and ERPs are correlated in their relation to *Y*. For example, if $|\beta^{\mathrm{ERP\_bi}}_{(f,t,e)}| < |\beta^{\mathrm{ERP}}_{(t,e)}|$, it indicates that part of the relation of probe-evoked voltage to *Y* is best captured by means of oscillatory power. Inversely, if $\beta^{\mathrm{ERP\_bi}}_{(f,t,e)} = \beta^{\mathrm{ERP}}_{(t,e)}$, it indicates that ERPs and oscillatory power independently correlate with *Y*.

Fig. 5A plots β^{pow} at electrode P3, indicating that from 250 to 500 ms after probe, target probes elicit greater 4-Hz power than do lures. Fig. 5B plots β^{ERP}, indicating that target probes elicit greater voltage than do lures from 200 to 300 ms after probe, and lures elicit greater voltage than do targets from 400 to 600 ms after probe. To determine if the oscillatory and ERP target–lure effects correlate at each time point, Figs. 5C and D plot $\beta^{\mathrm{pow\_bi}}$ and $\beta^{\mathrm{ERP\_bi}}$. $\beta^{\mathrm{pow\_bi}}$ and $\beta^{\mathrm{ERP\_bi}}$ show the same trends as β^{pow} and β^{ERP}, indicating that β's value did not vary according to whether it was computed in the univariate (Eqs. (3) and (4)) or bivariate (Eq. (5)) regressions. From this finding, we inferred that theta power changes do not fully account for the ERP target–lure effect.

Since ERP lag effects have been characterized previously (Golob and Starr, 2004), we were interested in determining if the oscillatory lag effects that we observed (e.g., Fig. 4C) were correlated with ERP effects. Fig. 6A compares ERP and oscillatory correlates of Lag, indicating that from 0 to 500 ms after probe, increased 2–4-Hz power occurred following recently viewed probes (small values of Lag). Fig. 6B indicates that, at 200 ms after probe, increased voltage is associated with larger values of Lag, as indicated by positive values of β^{ERP}. At this time point, however, $\beta^{\mathrm{ERP\_bi}}$ at 2–4 Hz is not significantly positive (Fig. 6D), indicating a correlation between the 2–4-Hz and ERP Lag effects.

ERP correlates of response confidence

Previous studies found that negative voltage deflections in response-locked ERPs were greatest in magnitude when subjects responded incorrectly (Luu et al., 2004; Pailing et al., 2000). Since our data indicated that RTQ can measure response confidence, we studied how response negativity related to confidence by studying response-locked ERPs for different values of RTQ. Fig. 7 plots the response-locked ERP for correct responses at a central electrode grouped by RTQ. ERPs are most negative when responses are slow, consistent with previous findings (Pailing et al., 2000).

Discussion

EEG working-memory studies have identified numerous relations between EEG oscillations and task manipulations. The present work replicates and extends several of these findings, by illustrating oscillatory patterns at different electrodes that simultaneously correlated with different task variables. These patterns were especially prevalent in the theta band, where we observed correlates of memory recognition, RT, and memory load at different electrodes and after-probe latencies. These observations indicate that although theta oscillations are present in widespread cortical regions, their functional role varies throughout the cortex—consistent with observations of multiple local cortical theta generators (Raghavachari et al., 2006).

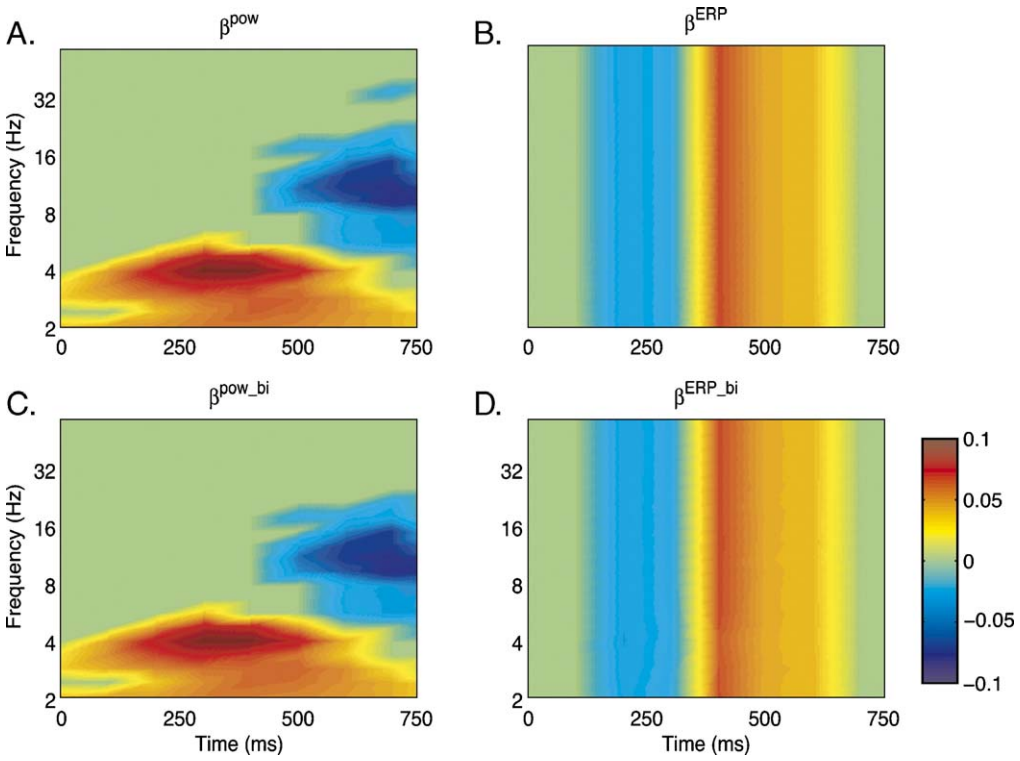

Fig. 5. Distinguishing oscillatory and ERP correlates of TL (βs from Eqs. (3), (4), and (5) at P3, substituting TL for Y). β plotted as 0 (green) when corresponding $P \geq 0.01$. (A) β^{pow} (Eq. (3)). (B) β^{ERP} (Eq. (4)). (C) β^{pow_bi} (Eq. (5)). (D) β^{ERP_bi} (Eq. (5)).

Our data indicate that left-parietal theta relates to memory recognition (Fig. 2). Left-parietal theta power initially (300 ms after probe) correlated with the degree of match between the probe and memory contents (TLC); later (500 ms after probe), it was best predicted by whether the probe was a target or lure (TL). We analyzed whether this theta target–lure effect was similar to the ERP target–lure effect, and found that they were not directly related, consistent with previous reports (Klimesch et al., 2000). ERPs result from a complex pattern of power and phase dynamics at a range of frequencies, but our analysis was only designed to distinguish power changes at single frequencies that affect ERP amplitude. Thus, we cannot rule out the possibility that theta

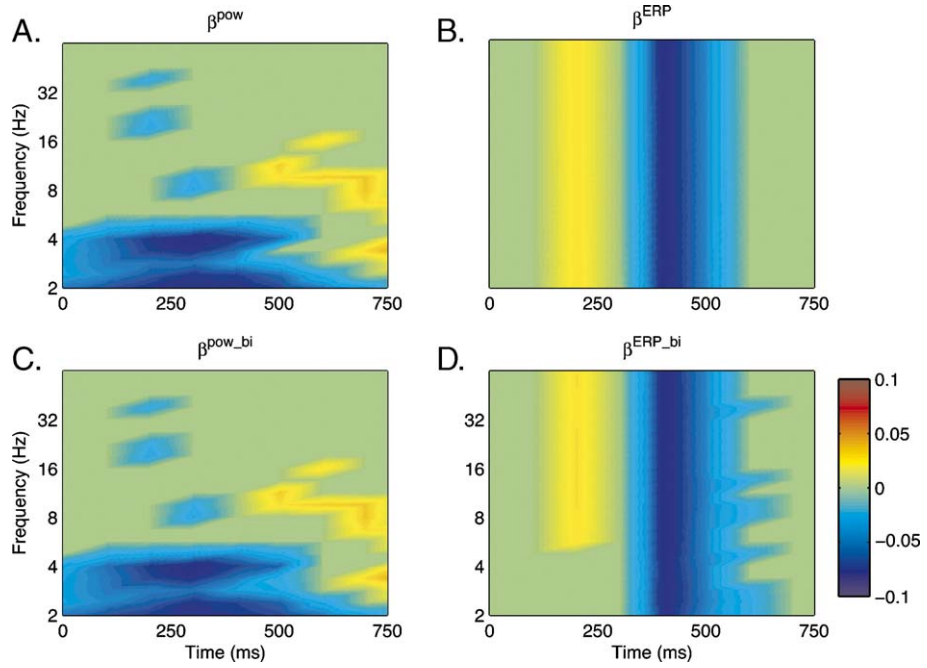

Fig. 6. Distinguishing oscillatory and ERP correlates of Lag (βs from Eqs. (3), (4), and (5) at PO7, substituting Lag for Y). β plotted as 0 (green) when corresponding $P \geq 0.01$. (A) β^{pow} (Eq. (3)). (B) β^{ERP} (Eq. (4)). (C) β^{pow_bi} (Eq. (5)). (D) β^{ERP_bi} (Eq. (5)).

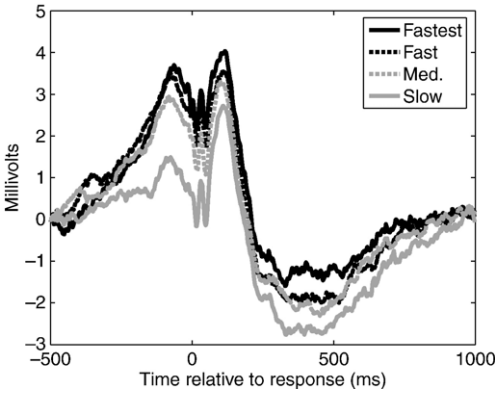

Fig. 7. RTQ-grouped response-locked ERPs. Response-locked ERPs for correct responses grouped by RTQ at electrode 107 (immediately right-anterior to CZ). Recordings are baseline corrected to voltage 500 ms before response.

oscillations relate to the ERP target–lure effect in a manner that is beyond the scope of our analysis. Nonetheless, both the ERP and theta target–lure effects are present at left-parietal electrodes 300 ms after probe, further implicating electrical activity recorded in this region in memory recognition.

Our observations relating left-parietal theta to memory recognition should not be interpreted as evidence that left-parietal theta is exclusive to working memory. In fact, recent work has described a similar left-parietal theta-power increase 300–500 ms after viewing open-class words (nouns, verbs, or adjectives) compared to viewing closed-class words (determiners, conjunctions, or prepositions) (Bastiaansen et al., 2005). Since these patterns have similar spatial and temporal characteristics, it seems reasonable to hypothesize that both patterns result from a more general phenomenon relating left-parietal theta to memory retrieval. Other studies observed that, in addition to theta, gamma power increased following target stimuli, compared with lures, in long-term recognition tasks (Gruber et al., 2004; Düzel et al., 2003). Since our analyses did not reveal this pattern, we hypothesize that gamma's relation to stimulus recognition is specific to tasks with long retention intervals.

Dual-process models of human memory generally assume the existence of neural correlates of familiarity and recollection (Norman and O'Reilly, 2003; Yonelinas, 2002). The neural-familiarity signal is a graded measure of the match between a stimulus and memory contents, whereas recollection is an all-or-none signal reflecting retrieval of the details of a stimulus. One interpretation of our findings suggests that left-parietal theta ~300 ms after probe could be a familiarity signal, because it correlated with TLC. Likewise, the ~500-ms left-parietal TL effect could be a correlate of recollection. Consistent with this interpretation, the oscillatory correlates of TLC and TL have time courses similar to observed ERP correlates of familiarity and recollection (Curran, 2000).

Previous studies demonstrated that central or frontal theta power related both to task difficulty (Gevins et al., 1997; Jensen and Tesche, 2002) and to response-related error processing (Luu et al., 2004). These observations, and the present findings, are consistent with central theta power relating to decision making. Figs. 3A and B illustrate that central theta (~7 Hz) power increased after probe onset and decreased before the response. This pattern correlated best with RTQ (negative values of β^{RTQ} in Fig. 1H), indicating that central theta related best to decision making rather than to stimuli manipulation. Consistent with this pattern, the anterior cingulate cortex, which underlies central electrodes, has been implicated in decision making via functional imaging studies (Botvinick et al., 2004).

Recent work found that increased theta power during incorrect responses related to the ERP error-related negativity (ERN) pattern (Luu et al., 2004). This pattern is consistent with theta relating to decision difficulty, because incorrect responses are associated with decreased confidence (and increased RTs). Since we observed that central theta power correlated with response confidence, it is also possible that the ERN related most directly to response confidence (rather than to error processing). We directly studied this by examining response-locked ERPs in correct trials (Fig. 7), and found that voltage was most negative for slow responses, consistent with previous findings (Pailing et al., 2000).

When we examined the relation between oscillatory power and memory load (e.g., Fig. 4A), we found that theta power decreased with increasing memory load: Fig. 1 shows that, at widespread electrodes, β^{LL} is negative at 4 Hz. This finding is opposite to the trend suggested by a previous study that analyzed the retention interval (Jensen and Tesche, 2002). This difference indicates that EEG oscillations can relate differently to behavior during distinct portions of the task. Moreover, this behavior-related power decrease exemplifies how oscillations can relate to behavior via both power increases, as is commonly seen in the theta band (Fig. 2), and power decreases, as is seen in the inverse relation between alpha power and attention (Pfurtscheller et al., 1996).

One version of a recent theoretical working-memory model suggested that the positive correlation between RT and memory load (Sternberg, 1966) is caused by an increase in theta's wavelength in proportion to the number of items stored in memory (Jensen and Lisman, 1998). Thus, this model predicts that theta's frequency would decrease with increasing memory load (LL). In our analyses, this pattern would result in negative values of β^{LL} at the upper part of the theta frequency range (~8 Hz) and positive values of β^{LL} at the lower end (~4 Hz). Since our analyses found negative values of β^{LL} at 4 Hz, they do not support this model.

Although our data do not demonstrate behavior-related EEG frequency shifts at individual electrodes, we did observe that different frequencies within the 4–8-Hz theta band best correlated with behavior across brain regions. Fig. 1H indicates that β^{RTQ} was greatest at central electrodes at ~7 Hz; Fig. 1D shows that β^{TL} was greatest in left-parietal regions at ~4 Hz. These theta-frequency differences could be explained by regional differences in neural structure (Buzsáki and Draguhn, 2004).

We also observed correlates of behavior in oscillations at frequencies outside the theta band: the left-parietal Lag effect (see Fig. 4C) is best characterized as a 2-Hz oscillatory effect but is also visible in ERPs. This finding indicates that previous observations of ERP serial-position effects (Golob and Starr, 2004) may also relate to phase-locked delta activity. In the alpha band, we found that oscillatory power ~700 ms after probe was greatest for fast RTs (Fig. 1), indicating that alpha power increased after subjects had responded and were not cognitively engaged. This is consistent with reports of alpha as a correlate of cortical idling (Pfurtscheller et al., 1996).

Finally, we found that increased gamma power after probe was correlated with slow RT (Fig. 3D). This relation is present immediately after the probe's onset, so it likely is related to attention or task vigilance rather than to probe processing. Although recent studies have also observed relations between gamma power and RT,

the reported direction of this relation varied depending on whether subjects could precisely predict stimuli onset: in studies in which subjects could predict when the cue would appear, increased gamma power was associated with fast responses (Gonzalez Andino et al., 2005); if subjects could not precisely predict the probe's onset, increased gamma power was present in slow trials (Jokeit and Makeig, 1994). We observed increased gamma power in trials in which subjects responded slowly, consistent with the fact that our probe onset was temporally jittered, preventing subjects from anticipating its exact onset.

Conclusions

We used a multivariate statistical framework to study how EEG oscillations related to working memory. Power of theta oscillations simultaneously correlated with different task variables: theta at left-parietal electrodes correlated with memory recognition, theta at central electrodes correlated with decision making, and theta at widespread electrodes correlated with memory load. In addition to theta, we also observed correlates of task variables in the delta, alpha, and gamma frequency bands. These patterns indicate that EEG oscillations can be used to map the functional roles of widespread brain regions. Our findings are the first to describe distinct patterns of theta oscillations that simultaneously relate to unique aspects of behavior. The range of patterns we observed indicates the functional diversity of human brain oscillations, and brings a new perspective to the debate over theta's role.

Acknowledgments

We would like to acknowledge Polly Johnsen for her editorial assistance, and Per Sederberg, Marieke van Vugt, and Sean Polyn for their helpful discussions on data analyses. For help with subject testing, we thank Daniel Blum, Sophie Boddington, Dan Collins, Tatsuko GoHollo, Megan Lipsett, Gabriel Matthews, Brion Woroch, and Brent Young. M.J.K. acknowledges support from National Institutes of Health research grants MH61975 and MH062196, NSF grant SBE0354378, and the Swartz Foundation. T.C. acknowledges support from National Institutes of Health research grant MH64812.

References

Bastiaansen, M., Hagoort, P., 2003. Event-induced theta responses as a window on the dynamics of memory. Cortex 39, 967–992.

Bastiaansen, M., van der Linden, M., ter Keurs, M., Dijkstra, T., Hagoort, P., 2005. Theta responses are involved in lexical-semantic retrieval during language processing. J. Cogn. Neurosci. 17, 530–541.

Botvinick, M., Cohen, J., Carter, C., 2004. Conflict monitoring and anterior cingulate cortex: an update. Trends Cogn. Sci. 8, 539–546.

Buzsáki, G., 2002. Theta oscillations in the hippocampus. Neuron 33 (3), 325–340.

Buzsáki, G., Draguhn, A., 2004. Neuronal oscillations in cortical networks. Science 304, 1926–1929.

Caplan, J.B., Madsen, J.R., Raghavachari, S., Kahana, M.J., 2001. Distinct patterns of brain oscillations underlie two basic parameters of human maze learning. J. Neurophysiol. 86, 368–380.

Caplan, J.B., Madsen, J.R., Schulze-Bonhage, A., Aschenbrenner-Scheibe, R., Newman, E.L., Kahana, M.J., 2003. Human theta oscillations related to sensorimotor integration and spatial learning. J. Neurosci. 23, 4726–4736.

Curran, T., 2000. Brain potentials of recollection and familiarity. Mem. Cogn. 28, 923–938.

de Araujo, D.B., Baffa, O., Wakai, R.T., 2002. Theta oscillations and human navigation: a magnetoencephalography study. J. Cogn. Neurosci. 14 (1), 70–78.

Delorme, A., Makeig, S., 2004. EEGLAB: an open source toolbox for analysis of single-trial EEG dynamics. J. Neurosci. Methods 134, 9–21.

Dien, J., 1998. Issues in the application of the average reference: review, critiques, and recommendations. Behav. Res. Meth. Instrum. Comput. 30, 34–43.

Düzel, E., Habib, R., Scott, B., Schoenfeld, A., Lobaugh, N., McIntosh, A.R., et al., 2003. A multivariate spatiotemporal analysis of electromagnetic time-frequency data of recognition memory. NeuroImage 18 (2), 185–197.

Ekstrom, A., Caplan, J., Ho, E., Shattuck, K., Fried, I., Kahana, M.J., 2005. Human hippocampal theta activity during virtual navigation. Hippocampus 15, 881–889.

Forrin, B., Cunningham, K., 1973. Recognition time and serial position of probed-item in short-term memory. J. Exp. Psychol. 99 (2), 272–279.

Friedman, D., Johnson, R., 2000. Event-related potential (ERP) studies of memory encoding and retrieval: a selective review. Microsc. Res. Tech. 51, 6–28.

Genovese, C.R., Lazar, N.A., Nichols, T.E., 2002. Thresholding of statistical maps in functional neuroimaging using the false discovery rate. NeuroImage 15, 870–878.

Gevins, A., Smith, M.E., McEvoy, L., Yu, D., 1997. High-resolution EEG mapping of cortical activation related to working memory: effects of task difficulty, type of processing, and practice. Cereb. Cortex 7 (4), 374–385.

Golob, E., Starr, A., 2004. Serial position effects in auditory event-related potentials during working memory retrieval. J. Cogn. Neurosci. 16, 40–52.

Gonzalez Andino, S., Michel, C., Thut, G., Landis, T., Peralto, de R.G., 2005. Prediction of response speed by anticipatory high-frequency (gamma band) oscillations in the human brain. Hum. Brain. Mapp. 24, 50–58.

Gruber, T., Matthias, M., 2005. Oscillatory brain activity dissociates between associative stimulus content in a repetition priming task in the human EEG. Cereb. Cortex 15, 109–116.

Gruber, T., Tsivilis, D., Montaldi, D., Müller, M., 2004. Induced gamma band responses: an early marker of memory encoding and retrieval. NeuroReport 15, 1837–1841.

Howard, M.W., Rizzuto, D.S., Caplan, J.C., Madsen, J.R., Lisman, J., Aschenbrenner-Scheibe, R., et al., 2003. Gamma oscillations correlate with working memory load in humans. Cereb. Cortex 13, 1369–1374.

Hwang, G., Jacobs, J., Geller, A., Danker, J., Sekuler, R., Kahana, M.J., 2005. EEG correlates of subvocal rehearsal in working memory. Behav. Brain Funct. 1, 20.

Jensen, O., Lisman, J.E., 1998. An oscillatory short-term memory buffer model can account for data on the Sternberg task. J. Neurosci. 18, 10688–10699.

Jensen, O., Tesche, C.D., 2002. Frontal theta activity in humans increases with memory load in a working memory task. Eur. J. Neurosci. 15, 1395–1399.

Jensen, O., Gelfand, J., Kounios, J., Lisman, J.E., 2002. Oscillations in the alpha band (9–12 Hz) increase with memory load during retention in a short-term memory task. Cereb. Cortex 12, 877–882.

Jokeit, H., Makeig, S., 1994. Different event-related patterns of gamma-band power in brain waves of fast- and slow-reacting subjects. Proc. Natl. Acad. Sci. U. S. A. 91 (14), 6339–6343.

Kahana, M.J., Sekuler, R., Caplan, J.B., Kirschen, M., Madsen, J.R., 1999. Human theta oscillations exhibit task dependence during virtual maze navigation. Nature 399, 781–784.

Kahana, M.J., Seelig, D., Madsen, J.R., 2001. Theta returns. Curr. Opin. Neurobiol. 11, 739–744.

Klimesch, W., Doppelmayr, M., Schwaiger, J., Winkler, T., Gruber, W., 2000. Theta oscillations and the ERP old/new effect: independent phenomena? Clin. Neurophysiol. 111, 781–793.

Klimesch, W., Hanslmayr, S., Sauseng, P., Gruber, W., Brozinsky, C.J., Kroll, N.E.A., et al., 2006. Oscillatory EEG correlates of episodic trace decay. Cereb. Cortex 16 (2), 280–290.

Luu, P., Tucker, D., Makeig, S., 2004. Frontal midline theta and the error-related negativity: neurophysiological mechanisms of action regulation. Clin. Neurophysiol. 115, 1821–1836.

Murdock, B.B., 1974. Human Memory: Theory and Data. Lawrence Erlbaum and Associates, Potomac, MD.

Norman, K.A., O'Reilly, R.C., 2003. Modeling hippocampal and neocortical contributions to recognition memory: a complementary learning systems approach. Psychol. Rev. 110, 611–646.

Pailing, P., Segalowitz, S., Davies, P., 2000. Speed of responding and the likelihood of error-like activity in correct trial ERPs. Psychophysiology, 37.

Pfurtscheller, G., Stancâk, A.J., Neuper, C., 1996. Event-related synchronization (ERS) in the alpha band—An electrophysiological correlate of cortical idling: a review. Int. J. Psychophysiol. 24, 39–46.

Raghavachari, S., Lisman, J.E., Tully, M., Madsen, J.R., Bromfield, E.B., Kahana, M.J., 2006. Theta oscillations in human cortex during a working memory task: evidence for local generators. J. Neurophysiol. 95 (3), 1630–1638.

Sternberg, S., 1966. High-speed scanning in human memory. Science 153, 652–654.

Sternberg, S., 1975. Memory scanning: new findings and current controversies. Q. J. Exp. Psychol. 27, 1–32.

Tallon-Baudry, C., Bertrand, O., Henaff, M.-A., Isnard, J., Fischer, C., 2005. Attention modulates gamma-band oscillations differently in the human lateral occipital cortex and fusiform gyrus. Cereb. Cortex 15 (5), 654–662.

Yonelinas, A., 2002. The nature of recollection and familiarity: a review of 30 years of research. J. Mem. Lang. 46, 441–517.